Current Pharmaceutical Biotechnology
Accepted for publication (May 2018), uncorrected

Metabolism of synthetic cannabinoid receptor agonists encountered in clinical casework: major *in vivo* phase I metabolites of JWH-007, JWH-019, JWH-203, JWH-307, UR-144, XLR-11, AM-2201, MAM-2201 and AM-694 in human urine using LC-MS/MS

Melanie Hutter,[a] Sebastian Broecker,[b] Stefan Kneisel,[a] Florian Franz,[a,c] Simon D. Brandt,[d] Volker Auwärter [a,*]

[a] *Institute of Forensic Medicine, Forensic Toxicology, Medical Center – University of Freiburg, Faculty of Medicine, University of Freiburg, Albertstr. 9, 79104 Freiburg, Germany*

[b] *Broeckers Solutions, Dyrotzer Straße 8, 13583 Berlin, Germany*

[c] *Hermann Staudinger Graduate School, University of Freiburg, Hebelstr. 27, 79104 Freiburg, Germany*

[d] *School of Pharmacy and Biomolecular Sciences, Liverpool John Moores University, Byrom Street, Liverpool L3 3AF, UK*

Short Title: **Major metabolites of nine synthetic cannabinoids in human urine**

*Corresponding author:
Volker Auwärter
Institute of Forensic Medicine
Forensic Toxicology
Albertstr. 9
79104 Freiburg
Germany
tel.: +49 761 203 6862
fax: +49 761 203 6826
E-mail: volker.auwaerter@uniklinik-freiburg.de

Abstract

Background: `Herbal mixtures` containing synthetic cannabinoid receptor agonists (SCRAs) are promoted as legal alternative to marihuana and are easily available via the Internet. Keeping analytical methods for the detection of these SCRAs up-to-date is a continuous challenge for clinicians and toxicologists due to the high diversity of the chemical structures and the frequent emergence of new compounds. Since many SCRAs are extensively metabolized, analytical methods used for urine testing require previous identification of the major metabolites of each compound.
Objective: The aim of this study was to identify the *in vivo* major metabolites of nine SCRAs (AM-694, AM-2201, JWH-007, JWH-019, JWH-203, JWH-307, MAM-2201, UR-144, XLR-11) for unambiguous detection of a drug uptake by analysis of urine samples.
Method: Positive urine samples from patients of hospitals, detoxification and therapy centers as well as forensic-psychiatric clinics were analyzed by means of liquid chromatography-tandem mass spectrometry (LC-MS/MS) and liquid chromatography-quadrupole time-of-flight mass spectrometry (LC-qToF-MS) for investigation of the *in vivo* major metabolites.
Results: For all investigated SCRAs, monohydroxylation, dihydroxylation and/or formation of the *N*-pentanoic acid metabolites were among the most abundant metabolites detected in human urine samples. Substitution of the fluorine atom was observed to be an important metabolic reaction for compounds carrying an *N*-(5-fluoropentyl) chain. Dealkylated metabolites were not detected *in vivo*.
Conclusion: The investigated metabolites facilitate the reliable detection of drug uptake by analysis of urine samples. For distinction between uptake of the fluorinated and the non-fluorinated analogs, the *N*-(4-hydroxypentyl) metabolite of the non-fluorinated analog was identified as a useful analytical target and consumption marker.

Keywords
synthetic cannabinoid receptor agonists; metabolism; LC-MS/MS; aminoalkylindoles; clinical toxicology; forensic toxicology.

Introduction

`Herbal mixtures` containing synthetic cannabinoid receptor agonists (SCRAs) have become a constant challenge for clinicians and toxicologists worldwide. New psychoactive substances (NPS) emerge frequently, in part, driven by implementation of control measures aiming at supply reduction [1-6]. However, a particular challenge encountered with the detection of SCRAs is the impressive diversity associated with the chemical structures and compound classes, which can make it difficult to keep analytical methods up to date. The development of methods used for the analysis of whole blood [7, 8], serum [9-14], hair [15, 16] or oral fluid [17-19] allows for the targeting of the parent compounds, whereas analytical methods used for urine testing require previous identification of the major metabolites since many SCRAs are extensively metabolized [12, 20-34]. Since the emergence of 'first generation' SCRAs, such as JWH-018 ((naphthalen-1-yl)(1-pentyl-1*H*-indol-3-yl)methanone) or JWH-073 ((1-butyl-1*H*-indol-3-yl)(naphthalen-1-yl)methanone) [35, 36], it has been observed that monohydroxylations, dihydoxylations and dealkylations are amongst the most commonly observed transformations followed by further oxidation to carboxylated products and conjugation [37]. During the last decade, the expansion into a wider range of chemically diverse chemical entities has resulted in the emergence of many new drugs on the NPS market [38-40]. However, despite this larger complexity, challenges can remain when faced with the identification of more 'established' derivatives.

This work presents an overview of major metabolites detected in human urine samples that originated from clinical/forensic casework involving the consumption of 'first' and 'second' generation SCRAs. The SCRAs investigated in this study were JWH-007, JWH-019, JWH-203, JWH-307, UR-144, XLR-11, AM-2201, MAM-2201 and AM-694 (Fig. 1).

Material and Methods

Chemicals and reagents

Methanol and 2-propanol were of gradient grade and were obtained from J.T. Baker (Deventer, Netherlands) and Carl Roth (Karlsruhe, Germany). *tert*-Butyl methyl ether and ammonium formate were supplied by Sigma-Aldrich (Steinheim, Germany), formic acid by Carl Roth (Karlsruhe, Germany) and *β*-glucuronidase (expressed by *Escherichia coli*, 140 U/mg at 37 °C) by Roche Diagnostics (Mannheim, Germany). Deionized water was prepared with a cartridge deionizer from Memtech (Moorenweis, Germany). The reference standards including AM-2201 *N*-(4-hydroxypentyl) metabolite, AM-2201 6-hydroxyindole metabolite, JWH-019 *N*-(6-hydroxyhexyl) metabolite, JWH-019 5-hydroxyindole metabolite, JWH-122 *N*-(5-hydroxypentyl) metabolite, JWH-122 *N*-(4-hydroxypentyl) metabolite, JWH-122 *N*-(5-carboxypentyl) metabolite, UR-144 *N*-(5-carboxypentyl) metabolite, UR-144 *N*-(5-hydroxypentyl) metabolite, UR-144 *N*-(4-hydroxypentyl) metabolite, UR-144 *N*-(5-carboxypentyl) metabolite and XLR-11 *N*-(4-hydroxypentyl) metabolite were provided by Cayman Chemicals (Ann Arbor, USA).

Mobile phase A consisted of water with 0.2 % formic acid and 2 mmol/L ammonium formate and was freshly prepared prior to analysis. Pure methanol was used as mobile phase B.

Authentic urine samples

Drug positive urine samples were obtained from patients of hospitals, detoxification and therapy centers as well as forensic-psychiatric clinics. All samples were paired with serum samples sent to our laboratory for detection of designer drug abuse and showed positive results for at least one SCRA related to the 'aminoalkylindole' subclass. At least five urine samples corresponding to positive serum samples for each SCRA were screened for major metabolites.

Urine sample preparation

Urine samples were extracted using the protocol described by Hutter *et al.* [31]. In brief: Liquid-liquid extraction of 0.5 mL urine was performed with *tert*-butyl methyl ether at pH 9 after enzymatic cleavage of glucuronides. The organic phase was evaporated and reconstituted in 100 µL mobile phase A/B (50:50, *v/v*).

Instrumentation and method

The extracted urine samples were analyzed by means of liquid chromatography-tandem mass spectrometry (LC-MS/MS) and liquid chromatography-quadrupol time-of-flight mass spectrometry (LC-qToF-MS). LC and MS settings were as described in a previous publication [31]. MassHunter Qualitative Analysis B.05.00 software was used for data analysis.
Drug positive urine samples were screened for major metabolites of the SCRAs found in the corresponding serum samples applying a similar approach as described by Hutter *et al.* [31]. The investigation covered the following phase I reactions: monohydroxylation, dihydroxylation, further oxidation steps, dealkylation, dehalogenation, epoxidation followed by rearrangement or hydrolysis and combinations of these reactions.

Results and Discussion

For identification of the major metabolites of the different compounds the anticipated fragment spectra of the metabolites were considered, based on the fragmentation of the parent compound. The examination of fragment masses allowed for the localization of the functional group introduced by the respective metabolic phase I reaction. For all metabolites with reference material available, matching of the retention times was evaluated. However, as there was no reference material for many of the metabolites, the exact position of the functional groups remains unclear in these cases.

(2-Methyl-1-pentyl-1H-indol-3-yl)(naphthalen-1-yl)methanone (JWH-007)

Figure 2 shows the multiple reaction monitoring (MRM) chromatogram (Fig. 2a) of a representative urine sample positive for metabolites of JWH-007 as well as the enhanced product ion spectra (EPI) of the parent compound (Fig. 2b) and its major metabolites (Fig. 2c-e). Two metabolites, carrying a hydroxyl group at the *N*-alkyl side chain, were detected as the most abundant metabolites in all analyzed urine samples (Fig. 2c). The fragment ion with a mass-to-charge ratio (*m/z*) of 244, which is 16 amu higher than the corresponding fragment ion *m/z* 228 of the parent compound, together with the unaltered indole fragment ion *m/z* 158 suggested hydroxylation at the *N*-pentyl side chain. Additionally, the *N*-pentanoic acid metabolite (Fig. 2d) originating from a further oxidation of the terminal hydroxylated *N*-alkyl side chain metabolite was detected among the major metabolites as well as a dihydroxylated metabolite (Fig. 2e), carrying both hydroxyl groups at the *N*-alkyl side chain.

(1-Hexyl-1H-indol-3-yl)(naphthalen-1-yl)methanone (JWH-019)

Two monohydroxylated and one *N*-hexanoic acid metabolites were identified as the major *in vivo* phase I biotransformation products of the SCRA JWH-019 (Fig. 3). Both monohydroxylated metabolites (Fig. 3c) with *m/z* 372 are characterized by unaltered naphthyl (fragment ions *m/z* 127, *m/z* 155) and indole moieties (*m/z* 144). The *m/z* 372>155 (quantifier) and *m/z* 372>127 (qualifier) transitions have been employed for the detection of the JWH-019 5-hydroxyindole metabolite in a method development study on the analysis of a range of metabolites in urine [41]. In combination with the fragment ion *m/z* 244, which is 16 amu higher than the corresponding fragment ion of the parent compound (*m/z* 228), monohydroxylation at the *N*-alkyl side chain at different positions for both compounds is suggested. The third metabolite detected in high abundance is the *N*-hexanoic acid metabolite (Fig. 3d) formed by a further oxidation of the terminal monohydroxylated metabolite. JWH-019 differs from JWH-018 in the length of the alkyl side chain only and the major metabolites of JWH-019 are in good accordance with the major metabolites described for JWH-018. However, no indole-hydroxylated metabolite was detected among the major metabolites as reported for JWH-018 [31]. In analogy to JWH-018, where a decarboxylation reaction of the carboxylated metabolite leads to metabolites typical for JWH-073 [31, 42], metabolites typical for JWH-018 were detected in urine samples positive for JWH-019 to a minor extent (data not shown). No JWH-018 was detected in the corresponding serum samples, therefore leading to the assumption that a decarboxylation reaction of the *N*-hexanoic acid metabolite of JWH-019 is responsible for the detected metabolites of JWH-018. By comparison with the available reference material the monohydroxylated metabolite eluting at retention time 8.0 min was identified as the JWH-019 *N*-(6-hydroxyhexyl) metabolite.

2-(2-Chlorophenyl)-1-(1-pentyl-1H-indol-3-yl)ethan-1-one (JWH-203)

The major metabolites of JWH-203 are depicted in Figure 4. Three monohydroxylated and one carboxylated compounds were detected as major metabolites. Two of the monohydroxylated metabolites (Fig. 4c) showed the same fragmentation pattern with unchanged indole (*m/z* 144) and 2-chlorobenzyl (*m/z* 125) moieties indicating hydroxylation at different positions of the *N*-alkyl side chain. In

both spectra the dehydrogenated fragment ion *m/z* 186 is more abundant than the fragment *m/z* 204 itself. The third monohydroxylated metabolite (Fig. 4d) shows hydroxylation at the indole moiety (*m/z* 160), which is not prone to further dehydrogenation reactions. Therefore, no fragment ion *m/z* 186 is detected in this case. In contrast, a predominant decarboxylated fragment ion (*m/z* 200) was detected in the spectrum of the *N*-pentanoic acid metabolite (Fig. 4e). As no reference standards for JWH-203 metabolites were available, further characterization of the monohydroxylated metabolites remains unclear. Interestingly, no dehalogenation was observed within the metabolic profiles of the analyzed urine sample. A comprehensive study on JWH-203 *in vivo* metabolism was also published by Kavanagh *et al.* whose results showed perfect accordance with the data obtained in this study [43].

[5-(2-Fluorophenyl)-1-pentyl-1H-pyrrol-3-yl](naphthalen-1-yl)methanone (JWH-307)

A notable structural feature in the SCRA JWH-307 is a 2-fluoro-phenyl pentyl pyrrol moiety substituting of the indole moiety. Figure 5 shows the major metabolites detected in the human urine samples. One of the two monohydroxylated metabolites detected at the 2-fluoro-phenyl pentyl pyrrol moiety showed highest abundance (Fig. 5a). In the ESI spectra (Fig. 5c) only the fragment ion *m/z* 230 was detected beside the unchanged naphthyl fragment ion *m/z* 155, deriving from a dehydrogenation of the theoretical fragment ion *m/z* 248 carrying the hydroxyl group. Further, a naphthyl dihydrodiol metabolite *m/z* 420 (indicated by the fragment ions *m/z* 189 and *m/z* 161) deriving from a hydrolysis of an epoxide intermediate was identified (Fig. 5d). The fragment ion *m/z* 171 is deriving from a loss of water of the fragment ion *m/z* 189 and a further elimination of CO leads to the fragment ion *m/z* 143. Additionally, two dihydroxylated metabolites were detected carrying the hydroxyl groups at the naphthyl (*m/z* 143 and *m/z* 171) and the 2-fluoro-phenyl pentyl pyrrol moiety (*m/z* 230), respectively. In comparison, Strano-Rossi *et al.* published an *in vitro* study about the identified phase I major metabolites of JWH-307 using rat liver slices [44]. They reported a monohydroxy, two ketone, one unsaturated and one dihydroxy compound to be the most abundant phase I metabolites identified. The supposed ω-1 monohydroxy metabolite might be identical to one of the monohydroxy metabolites detected during our study, while the other four reported metabolites did not correspond to any major metabolites identified in our study. Furthermore, there was no dihydrodiol metabolite identified *in vitro*, which occurred in high abundance *in vivo*. This comparison shows that *in vitro* results can be extremely different from the actual human *in vivo* metabolic profiles and *in silico* or *in vitro* predicted phase I metabolites have to be confirmed by analysis of human urine samples.

(1-Pentyl-1H-indol-3-yl)(2,2,3,3-tetramethylcyclopropyl)methanone (UR-144)

Studies on the chemical characteristics and *in vitro* and *in vivo* studies of the metabolism of the SCRA UR-144 have been reported previously [45-49]. UR-144 and its isomers with an altered tetra methyl cyclopropyl moiety were found in herbal mixtures as well as after thermal degradation and can be distinguished by their chromatographic behavior as well as by their differences observed in the product ion

mass spectra. No product ions typical for the tetra methyl cyclopropyl moiety (*m/z* 125 and *m/z* 97) were detected in the ESI mass spectra of the isomers of UR-144 [45, 46]. Different metabolites monohydroxylated at the *N*-alkyl side chain, the indole moiety or the tetra methyl cyclopropyl moiety of UR-144, respectively, as well as two monohydroxylated metabolites of the ring opened isomer were reported to be most abundant in human urine samples. Before suitable reference materials were commercially available, a hydroxyindole and hydroxypentyl metabolite was identified qualitatively during the course of an acute intoxication [50]. Additionally, a monohydroxylated hydrated metabolite of the ring opened isomer was detected in urine samples with high abundance [45, 46]. In urine samples analyzed in our laboratory, four monohydroxylated metabolites were identified as major metabolites of UR-144. One monohydroxylated metabolite of the ring-opened isomer was the most abundant metabolite showing monohydroxylation at the *N*-alkyl side chain (*m/z* 230) (Fig. 6c). The open ring form is suggested since the product ions *m/z* 125 or *m/z* 97 were not detected (Fig 6c). Additionally, two *N*-alkyl side chain hydroxylated metabolites (*m/z* 230) with an unaltered tetra methyl cyclopropyl ring indicated by the presence of *m/z* 125 (Fig. 6d) as well as a monohydroxylated metabolite at the tetra methyl cyclopropyl moiety (*m/z* 214) (Fig. 6e) were detected. Further chromatographic separation of the peak at 7.9 min and comparison with the reference material revealed two *N*-alkyl side chain hydroxylated metabolites, namely the UR-144 *N*-(4-hydroxypentyl) showing the higher abundance and the *N*-(5-hydroxypentyl) metabolite (data not shown). Neither the parent compound UR-144 nor the hydrated ring opened isomer or the ring opened isomer itself were detected in any of the urine samples. In summary, the results of our study are in agreement with the major metabolites reported in scientific literature [49, 51] and it was possible to confirm the structures of two of these monohydroxylated metabolites.

[1-(5-Fluoropentyl)-1H-indol-3-yl](2,2,3,3-tetramethylcyclopropyl)methanone (XLR-11)

The 5-fluoropentyl analog of UR-144, namely XLR-11, firstly appeared in herbal mixtures in November 2012 on the European market. In analogy to UR-144 in herbal mixtures as well as in serum samples a ring-opened isomer of XLR-11 can be detected beside the XLR-11 itself indicated by the lacking fragments *m/z* 125 and *m/z* 97 [52, 53]. Hence, a similar metabolism pattern to UR-144 is suspected (Fig. 7). In contrast to UR-144 the *N*-(5-hydroxypentyl) metabolite was detected with high abundance and only small traces of the *N*-(4-hydroxypentyl) metabolite of UR-144 were found. Therefore, similar to what has been observed for AM-2201 and MAM-2201 (see below), the *N*-(5-hydroxypentyl) metabolite can be used as a marker to distinguish between UR-144 and XLR-11 consumption [54, 55]. Only small traces of the ring opened isomer as well as the hydrated isomer *m/z* 348 and no XLR-11 were detected in any of the urine samples analyzed. Further studies performed by Wohlfarth *et al.*, Kanamori *et al.*, Nielsen *et al.*, Jang *et al.* Cannaert *et al*. and Richter *et al*. showed comparable qualitative results [49, 51-53, 56, 57].

[1-(5-Fluoropentyl)-1H-indol-3-yl](naphthalen-1-yl)methanone (AM-2201)

First detected in 2011, fluorinated analogs of already known SCRAs appeared on the market. AM-2201, the 5-fluoropentyl analog of JWH-018 was detected in an herbal mixture in Europe in June 2011 for the first time. Metabolism of AM-2201 was already reported in previous studies [45, 54, 58-61] One 5-fluoropentyl chain and one indole hydroxylated metabolite of AM-2201 were identified as the major metabolites of AM-2201 in our study (Fig. 8). Comparison of retention times of the identified compounds with the available reference material led to their assignment as the AM-2201 *N*-(4-hydroxy-5-fluoropentyl) metabolite (Fig. 8c), one hydroxypentyl metabolite targeted for urinary analysis [61, 62], and the AM-2201 6-OH-indole metabolite (Fig. 8d), respectively. Interestingly, metabolites typical for JWH-018 were found among the major metabolites of AM-2201 even after oral administration of pure AM-2201 [54]. The abundance of the JWH-018 metabolites deriving from AM-2201 however was higher than those of the metabolites still carrying the fluorine atom (Fig. 9).

[1-(5-Fluoropentyl)-1H-indol-3-yl](4-methylnaphthalen-1-yl)methanone (MAM-2201)

Simultaneously with AM-2201, the 5-fluoropentyl analog of JWH-122, called MAM-2201, appeared on the European market. Major metabolites of JWH-122 showed monohydroxylation at the pentyl side chain, the naphthyl and the indole moiety with the pentyl hydroxylated metabolite showing the highest abundance [31]. Hydroxylations at the indole (Fig. 10c) as well as at the naphthyl moieties (Fig. 10d) were detected among the major metabolites in all urine samples investigated. Furthermore, the *N*-pentanoic acid metabolite was identified (Fig. 10e) which was further confirmed by comparison with the JWH-122 *N*-pentanoic acid metabolite reference material. Apparently, also in case of MAM-2201, a oxidative defluorination reaction leading to the metabolites of JWH-122 takes place in humans. In analogy to AM-2201, the JWH-122 *N*-(5-hydroxypentyl) metabolite but not the JWH-122 *N*-(4-hydroxypentyl) metabolite, which is one of the major metabolites of JWH-122, was detected in the authentic urine samples (Fig. 10 peak f) [54]. JWH-122 was not detected in any of the serum samples corresponding to the analyzed urine samples supporting the suggestion that the metabolites of JWH-122 detected in the urine samples derive from biotransformation of MAM-2201. These observations are consistent with results from a metabolism study published by Jang *et al*. [55]. The MAM-2201 *N*-(4-hydroxypentyl) metabolite was detected and used for targeted analysis by Kronstrand *et al*. [63] and Knittel *et al*. [62].

[1-(5-Fluoropentyl)-1H-indol-3-yl](2-iodophenyl)methanone (AM-694)

The SCRA AM-694 is also characterized by the presence of an *N*-(5-fluoropentyl) tail. As there have been only a small number of urine samples with paired serum samples positive for AM-694 for confirmation of drug uptake the metabolism of this SCRA was investigated by a controlled self-experiment where an adult volunteer (45 year old Caucasian male, 75 kg) ingested 5 mg of pure crystalline AM-694 in a gelatine capsule orally. Urine samples were collected for the following days and analyzed as described above. The volunteer experienced no physical or mental effects at any stage of the experiment. The major metabolites of AM-694 detected in this experiment are depicted in Figure 11. Two metabolites hydroxylated at the *N*-alkyl

chain still carrying the fluoro atom were identified (Fig. 11c) as well as one metabolite formed by oxidative defluorination (Fig. 11d). Dehydration of the product ion at *m/z* 204 carrying the hydroxyl group led to the ion at *m/z* 186 that showed a higher abundance in the EPI spectra as the hydroxylated fragment ion itself. Furthermore, the *N*-pentanoic acid metabolite formed by further oxidation of the *N*-(hydroxypentyl) metabolite was identified (Fig. 11e). Since the analyzed urine samples derived from a self-experiment, where only pure AM-694 was ingested, these results along with observations within the metabolic patterns of the other fluorinated SCRAs above (AM-2201, MAM-2201 and XLR-11), confirm that oxidative defluorination takes place during biotransformation of these compounds in humans. The observations made were consistent with those reported by Grigoryev *et al.* [29] and Bertol *et al.* [64] who reported on the analysis of urine samples obtained from intoxication cases.

Limitations of the study

(I) Oxidative metabolism is mainly catalyzed by different CYP 450 isoenzymes as already shown for other SCRAs. Several CYP isoforms (e.g. CYP2D6 and CYP2C19) are known to be polymorphically expressed. This fact might influence individual metabolic profiles and could have clinical relevance e.g. in case of drug-drug interactions. However, as our study mainly focused on the detection of SCRA use by urine analysis, we refrained from experimental identification of the isoenzymes involved in the metabolic reactions. Moreover, the abundance of detected drug metabolites depends on many other factors like consumption behavior (e.g. frequency and time period of consumption; route and amount of drug uptake) and time distance to the last drug uptake. However, reliable information about a subject´s consumption behavior or phenotype is lacking in most clinical or forensic cases. Whenever possible, individual variation of the metabolic profiles was taken into account by analysis of several positive urine samples.
(II) Since commercial reference standards were not available for most metabolites, qualitative classification as ‘major’ or ‘minor’ metabolite was based on peak heights. Although similar response factors can be assumed for structurally similar phase I metabolites of a SCRA, differences in extraction efficiency, ionization efficiency, fragmentation efficiency, and matrix effects might strongly bias the signal intensities.

Conclusion

For all investigated SCRAs encountered during casework, monohydroxylation, dihydroxylation and/or formation of the carboxylic acid were among the main metabolic reactions according to the metabolites detected in human urine samples. For all SCRAs investigated carrying an *N*-(5-fluoropentyl) chain, a metabolic substitution of the fluorine atom was observed and in cases where reference material was available, these biotransformation products were identified as the *N*-(5-hydroxypentyl) metabolite of the non-fluorinated analog, leading to common major metabolites of these analogs. In contrast, the highly abundant *N*-(4-hydroxypentyl) metabolites of the non-fluorinated analogs were not formed from the *N*-(5-fluoropentyl) analogs and can therefore serve as a useful biomarker for distinction between uptake of the fluorinated and the non-fluorinated analogs. Dealkylated

metabolites were not detected by the applied EPI scan method in the *in vivo* samples. As reference standards for the metabolites of many aminoalkylindoles were not yet available at the time of these investigations, the exact positions of the hydroxylation sites remained unclear, although some of the positions might be suggested by considering relative retention time differences in comparison with known metabolic profiles of structurally related compounds.

Acknowledgments

The authors would like to thank the EU-Commission (JUST/2011/DPIP/AG/3597), the German Ministry of Health and the City of Frankfurt (Main), Germany, for funding the project ‘Spice II Plus’. Furthermore, the study was kindly supported financially by the ‘Konrad-Händel-Stiftung’.

References

[1] Uchiyama N, Kawamura M, Kikura-Hanajiri R, Goda Y. URB-754: A new class of designer drug and 12 synthetic cannabinoids detected in illegal products. Forensic Science International, 2013; 227: 21-32.

[2] Nakajima J, Takahashi M, Nonaka R, Seto T, Suzuki J, Yoshida M, Kanai C, Hamano T. Identification and quantitation of a benzoylindole (2-methoxyphenyl)(1-pentyl-1*H*-indol-3-yl)methanone and a naphthoylindole 1-(5-fluoropentyl-1*H*-indol-3-yl)-(naphthalene-1-yl)methanone (AM-2201) found in illegal products obtained via the Internet and their cannabimimetic effects evaluated by in vitro [^{35}S]GTPγS binding assays. Forensic Toxicology, 2011; 29: 132-141.

[3] Nakajima J, Takahashi M, Seto T, Kanai C, Suzuki J, Yoshida M, Hamano T. Identification and quantitation of two benzoylindoles AM-694 and (4-methoxyphenyl)(1-pentyl-1H-indol-3-yl)methanone, and three cannabimimetic naphthoylindoles JWH-210, JWH-122, and JWH-019 as adulterants in illegal products obtained via the Internet. Forensic Toxicology, 2011; 29: 95-110.

[4] Hudson S, Ramsey J, King L, Timbers S, Maynard S, Dorgan PI, Wood DM. Use of high-resolution accurate mass spectrometry to detect reported and previously unreported cannabinomimetics in "herbal high" products. Journal of Analytical Toxicology, 2010; 34: 252-260.

[5] Bononi M, Belgi P, Tateo F. Analytical data for identification of the cannabimimetic phenylacetylindole JWH-203. Journal of Analytical Toxicology, 2011; 35: 360-363.

[6] Ernst L, Kruger K, Lindigkeit R, Schiebel HM, Beuerle T. Synthetic cannabinoids in "spice-like" herbal blends: First appearance of JWH-307 and recurrence of JWH-018 on the German market. Forensic Science International, 2012; 222: 216-222.

[7] Kacinko SL, Xu AL, Homan JW, McMullin MM, Warrington DM, Logan BK. Development and validation of a liquid chromatography-tandem mass spectrometry method for the identification and quantification of JWH-018, JWH-073, JWH-019, and JWH-250 in human whole blood. Journal of Analytical Toxicology, 2011; 35: 386-393.

[8] Shanks KG, Dahn T, Terrell AR. Detection of JWH-018 and JWH-073 by UPLC-MS-MS in postmortem whole blood casework. Journal of Analytical Toxicology, 2012; 36: 145-152.

[9] Ammann J, McLaren JM, Gerostamoulos D, Beyer J. Detection and quantification of new designer drugs in human blood: part 1. Synthetic cannabinoids. Journal of Analytical Toxicology, 2012; 36: 372-380.

[10] Dresen S, Kneisel S, Weinmann W, Zimmermann R, Auwärter V. Development and validation of a liquid chromatography-tandem mass spectrometry method for the quantitation of synthetic cannabinoids of the aminoalkylindole type and methanandamide in serum and its application to forensic samples. Journal of Mass Spectrometry, 2011; 46: 163-171.

[11] Kneisel S, Auwärter V. Analysis of 30 synthetic cannabinoids in serum by liquid chromatography-electrospray ionization tandem mass spectrometry after liquid-liquid extraction. Journal of Mass Spectrometry, 2012; 47: 825-835.

[12] Moller I, Wintermeyer A, Bender K, Jubner M, Thomas A, Krug O, Schänzer W, Thevis M. Screening for the synthetic cannabinoid JWH-018 and its major metabolites in human doping controls. Drug Testing and Analysis, 2011; 3: 609-620.

[13] Teske J, Weller JP, Fieguth A, Rothamel T, Schulz Y, Troger HD. Sensitive and rapid quantification of the cannabinoid receptor agonist naphthalen-1-yl-(1-pentylindol-3-yl)methanone (JWH-018) in human serum by liquid chromatography-tandem mass spectrometry. Journal of Chromatography B-Analytical Technologies in the Biomedical and Life Sciences, 2010; 878: 2659-2663.

[14] Dziadosz M, Weller JP, Klintschar M, Teske J. Scheduled multiple reaction monitoring algorithm as a way to analyse new designer drugs combined with synthetic cannabinoids in human serum with liquid chromatography-tandem mass spectrometry. Journal of Chromatography B-Analytical Technologies in the Biomedical and Life Sciences, 2013; 929: 84-89.

[15] Salomone A, Gerace E, D'Urso F, Di Corcia D, Vincenti M. Simultaneous analysis of several synthetic cannabinoids, THC, CBD and CBN, in hair by ultra-high performance liquid chromatography tandem mass spectrometry. Method validation and application to real samples. Journal of Mass Spectrometry, 2012; 47: 604-610.

[16] Hutter M, Kneisel S, Auwärter V, Neukamm MA. Determination of 22 synthetic cannabinoids in human hair by liquid chromatography-tandem mass spectrometry. Journal of Chromatography B-Analytical Technologies in the Biomedical and Life Sciences, 2012; 903: 95-101.

[17] Coulter C, Garnier M, Moore C. Synthetic cannabinoids in oral fluid. Journal of Analytical Toxicology, 2011; 35: 424-430.

[18] Kneisel S, Auwärter V, Kempf J. Analysis of 30 synthetic cannabinoids in oral fluid using liquid chromatography-electrospray ionization tandem mass spectrometry. Drug Testing and Analysis, 2013; 5: 657-669.

[19] Strano-Rossi S, Anzillotti L, Castrignano E, Romolo FS, Chiarotti M. Ultra high performance liquid chromatography-electrospray ionization-tandem mass spectrometry screening method for direct analysis of designer drugs, "spice" and stimulants in oral fluid. Journal of Chromatography A, 2012; 1258: 37-42.

[20] Yanes EG, Lovett DP. High-throughput bioanalytical method for analysis of synthetic cannabinoid metabolites in urine using salting-out sample preparation and LC-MS/MS. Journal of Chromatography B-Analytical Technologies in the Biomedical and Life Sciences, 2012; 909: 42-50.

[21] Chimalakonda KC, Moran CL, Kennedy PD, Endres GW, Uzieblo A, Dobrowolski PJ, Fifer EK, Lapoint J, Nelson LS, Hoffman RS, James LP, Radominska-Pandya A, Moran JH. Solid-phase extraction and quantitative measurement of omega and omega-1 metabolites of JWH-018 and JWH-073 in human urine. Analytical Chemistry, 2011; 83: 6381-6388.

[22] de Jager AD, Warner JV, Henman M, Ferguson W, Hall A. LC-MS/MS method for the quantitation of metabolites of eight commonly-used synthetic cannabinoids in human urine - an Australian perspective. Journal of Chromatography B-Analytical Technologies in the Biomedical and Life Sciences, 2012; 897: 22-31.

[23] Dowling G, Regan L. A method for CP 47, 497 a synthetic non-traditional cannabinoid in human urine using liquid chromatography tandem mass spectrometry. Journal of Chromatography B-Analytical Technologies in the Biomedical and Life Sciences, 2011; 879: 253-259.

[24] Wohlfarth A, Scheidweiler KB, Chen XH, Liu HF, Huestis MA. Qualitative confirmation of 9 synthetic cannabinoids and 20 metabolites in human urine using LC-MS/MS and library search. Analytical Chemistry, 2013; 85: 3730-3738.

[25] Moran CL, Le VH, Chimalakonda KC, Smedley AL, Lackey FD, Owen SN, Kennedy PD, Endres GW, Ciske FL, Kramer JB, Kornilov AM, Bratton LD, Dobrowolski PJ, Wessinger WD, Fantegrossi WE, Prather PL, James LP, Radominska-Pandya A, Moran JH. Quantitative measurement of JWH-018

and JWH-073 metabolites excreted in human uUrine. Analytical Chemistry, 2011; 83: 4228-4236.

[26] Diao X, Huestis MA. Approaches, challenges, and advances in metabolism of new synthetic cannabinoids and identification of optimal urinary marker metabolites. Clinical Pharmacology and Therapeutics 2017; 101: 239-253.

[27] Beuck S, Möller I, Thomas A, Klose A, Schlörer N, Schänzer W, Thevis M. Structure characterisation of urinary metabolites of the cannabimimetic JWH-018 using chemically synthesised reference material for the support of LC-MS/MS-based drug testing. Analytical and Bioanalytical Chemistry, 2011; 401: 493-505.

[28] Grigoryev A, Kavanagh P, Melnik A. The detection of the urinary metabolites of 3-[(adamantan-1-yl)carbonyl]-1-pentylindole (AB-001), a novel cannabimimetic, by gas chromatography-mass spectrometry. Drug Testing and Analysis, 2012; 4: 519-524.

[29] Grigoryev A, Kavanagh P, Melnik A. The detection of the urinary metabolites of 1-[(5-fluoropentyl)-1H-indol-3-yl]-(2-iodophenyl)methanone (AM-694), a high affinity cannabimimetic, by gas chromatography - mass spectrometry. Drug Testing and Analysis, 2013; 5: 110-115.

[30] Grigoryev A, Melnik A, Savchuk S, Simonov A, Rozhanets V. Gas and liquid chromatography-mass spectrometry studies on the metabolism of the synthetic phenylacetylindole cannabimimetic JWH-250, the psychoactive component of smoking mixtures. Journal of Chromatography B-Analytical Technologies in the Biomedical and Life Sciences, 2011; 879: 2519-2526.

[31] Hutter M, Broecker S, Kneisel S, Auwärter V. Identification of the major urinary metabolites in man of seven synthetic cannabinoids of the aminoalkylindole type present as adulterants in herbal mixtures' using LC-MS/MS techniques. Journal of Mass Spectrometry, 2012; 47: 54-65.

[32] Kavanagh P, Grigoryev A, Melnik A, Simonov A. The Identification of the urinary metabolites of 3-(4-methoxybenzoyl)-1-pentylindole (RCS-4), a novel cannabimimetic, by gas chromatography mass spectrometry. Journal of Analytical Toxicology, 2012; 36: 303-311.

[33] Sobolevsky T, Prasolov I, Rodchenkov G. Detection of JWH-018 metabolites in smoking mixture post-administration urine. Forensic Science International, 2010; 200: 141-147.

[34] Castaneto MS, Wohlfarth A, Desrosiers NA, Hartman RL, Gorelick DA, Huestis MA. Synthetic cannabinoids pharmacokinetics and detection methods in biological matrices. Drug Metabolism Reviews, 2015; 47: 124-174.

[35] European Monitoring Centre for Drugs and Drug Addiction (EMCDDA). Understanding the 'Spice' phenomenon. Lisbon, Portugal. Available at: http://www.emcdda.europa.eu/system/files/publications/537/Spice-Thematic-paper-final-version.pdf, 2009.

[36] United Nations Office on Drugs and Crime (UNODC). Synthetic cannabinoids in herbal products. UNODC, Vienna, Austria. Available at: https://www.unodc.org/documents/scientific/Synthetic_Cannabinoids.pdf, 2011.

[37] Chimalakonda KC, Bratton SM, Le VH, Yiew KH, Dineva A, Moran CL, James LP, Moran JH, Radominska-Pandya A. Conjugation of synthetic cannabinoids JWH-018 and JWH-073, metabolites by human UDP-glucuronosyltransferases. Drug Metabolism and Disposition, 2011; 39: 1967-1976.

[38] European Monitoring Centre for Drugs and Drug Addiction (EMCDDA). Synthetic cannabinoids in Europe (Perspectives on drugs). Lisbon, Portugal. Available at: http://www.emcdda.europa.eu/system/files/publications/2753/POD_Synthetic%20cannabinoids_0.pdf, 2017.

[39] European Monitoring Centre for Drugs and Drug Addiction (EMCDDA). European Drug Report 2017. Trends and Developments. Publications Office of the European Union, Luxembourg. Available at: http://www.emcdda.europa.eu/system/files/publications/4541/TDAT17001ENN.pdf, 2017.

[40] United Nations Office on Drugs and Crime (UNODC). Market analysis of new synthetic drugs. Amphetamine-type stimulants, new psychoactive substances. World Drug Report 2017. UNODC, Vienna, Austria. Available at: http://www.unodc.org/wdr2017/field/Booklet_4_ATSNPS.pdf, 2017.

[41] Scheidweiler KB, Huestis MA. Simultaneous quantification of 20 synthetic cannabinoids and 21 metabolites, and semi-quantification of 12 alkyl hydroxy metabolites in human urine by liquid chromatography-tandem mass spectrometry. J. Chromatogr. A, 2014; 1327: 105-117.

[42] Lovett DP, Yanes EG, Herbelin TW, Knoerzer TA, Levisky JA. Structure elucidation and identification of a common metabolite for naphthoylindole-based synthetic cannabinoids using LC-TOF and comparison to a synthetic reference standard. Forensic Science International, 2013; 226: 81-87.

[43] Kavanagh P, Grigoryev A, Melnik A, Savchuk S, Simonov A, Rozhanets V. Detection and tentative identification of urinary phase I metabolites of

phenylacetylindole cannabimimetics JWH-203 and JWH-251, by GC-MS and LC-MS/MS. Journal of Chromatography B, 2013; 934: 102-8.

[44] Strano-Rossi S, Anzillotti L, Dragoni S, Pellegrino RM, Goracci L, Pascali VL, Cruciani G. Metabolism of JWH-015, JWH-098, JWH-251, and JWH-307 in silico and in vitro: a pilot study for the detection of unknown synthetic cannabinoids metabolites. Analytical and Bioanalytical Chemistry, 2014; 406: 3621-3636.

[45] Sobolevsky T, Prasolov I, Rodchenkov G. Detection of urinary metabolites of AM-2201 and UR-144, two novel synthetic cannabinoids. Drug Testing and Analysis, 2012; 4: 745-753.

[46] Grigoryev A, Kavanagh P, Melnik A, Savchuk S, Simonov A. Gas and liquid chromatography-mass spectrometry detection of the urinary metabolites of UR-144 and its major pyrolysis product. Journal of Analytical Toxicology, 2013; 37: 265-276.

[47] Kavanagh P, Grigoryev A, Savchuk S, Mikhura I, Formanovsky A. UR-144 in products sold via the Internet: identification of related compounds and characterization of pyrolysis products. Drug Testing and Analysis, 2013; 5: 683-692.

[48] Adamowicz P, Zuba D, Sekula K. Analysis of UR-144 and its pyrolysis product in blood and their metabolites in urine. Forensic Sci Int, 2013; 233: 320-7.

[49] Nielsen LM, Holm NB, Olsen L, Linnet K. Cytochrome P450-mediated metabolism of the synthetic cannabinoids UR-144 and XLR-11. Drug Testing and Analysis, 2016; 8: 792-800.

[50] Hermanns-Clausen M, Kneisel S, Hutter M, Szabo B, Auwärter V. Acute intoxication by synthetic cannabinoids - Four case reports. Drug Test. Anal., 2013; 5: 790-794.

[51] Cannaert A, Franz F, Auwärter V, Stove CP. Activity-based detection of consumption of synthetic cannabinoids in authentic urine samples using a stable cannabinoid reporter system. Anal. Chem., 2017; 89: 9527-9536.

[52] Kanamori T, Kanda K, Yamamuro T, Kuwayama K, Tsujikawa K, Iwata YT, Inoue H. Detection of main metabolites of XLR-11 and its thermal degradation product in human hepatoma HepaRG cells and human urine. Drug Testing and Analysis, 2015; 7: 341-345.

[53] Jang M, Kim IS, Park YN, Kim J, Han I, Baeck S, Yang W, Yoo HH. Determination of urinary metabolites of XLR-11 by liquid chromatography-

quadrupole time-of-flight mass spectrometry. Analytical and Bioanalytical Chemistry, 2016; 408: 503-516.

[54] Hutter M, Moosmann B, Kneisel S, Auwärter V. Characteristics of the designer drug and synthetic cannabinoid receptor agonist AM-2201 regarding its chemistry and metabolism. Journal of Mass Spectrometry, 2013; 48: 885-894.

[55] Jang M, Shin I, Yang W, Chang H, Yoo HH, Lee J, Kim E. Determination of major metabolites of MAM-2201 and JWH-122 in in vitro and in vivo studies to distinguish their intake. Forensic Science International, 2014; 244: 85-91.

[56] Wohlfarth A, Pang S, Zhu M, Gandhi AS, Scheidweiler KB, Liu HF, Huestis MA. First metabolic profile of XLR-11, a novel synthetic cannabinoid, obtained by using human hepatocytes and high-resolution mass spectrometry. Clinical Chemistry, 2013; 59: 1638-48.

[57] Richter LHJ, Maurer HH, Meyer MR. New psychoactive substances: studies on the metabolism of XLR-11, AB-PINACA, FUB-PB-22, 4-methoxy-α-PVP, 25-I-NBOMe, and meclonazepam using human liver preparations in comparison to primary human hepatocytes, and human urine. Toxicol. Lett., 2017; 280: 142-150.

[58] Moosmann B, Kneisel S, Girreser U, Brecht V, Westphal F, Auwärter V. Separation and structural characterization of the synthetic cannabinoids JWH-412 and 1-[(5-fluoropentyl)-1H-indol-3yl]-(4-methylnaphthalen-1-yl)methanone using GC-MS, NMR analysis and a flash chromatography system. Forensic Science International, 2012; 220: E17-E22.

[59] Jang M, Yang W, Shin I, Choi H, Chang H, Kim E. Determination of AM-2201 metabolites in urine and comparison with JWH-018 abuse. International Journal of Legal Medicine, 2014; 128: 285-294.

[60] Chimalakonda KC, Seely KA, Bratton SM, Brents LK, Moran CL, Endres GW, James LP, Hollenberg PF, Prather PL, Radominska-Pandya A, Moran JH. Cytochrome P450-Mediated Oxidative Metabolism of Abused Synthetic Cannabinoids Found in K2/Spice: Identification of Novel Cannabinoid Receptor Ligands. Drug Metabolism and Disposition, 2012; 40: 2174-2184.

[61] Wohlfarth A, Scheidweiler KB, Castaneto M, Gandhi AS, Desrosiers NA, Klette KL, Martin TM, Huestis MA. Urinary prevalence, metabolite detection rates, temporal patterns and evaluation of suitable LC-MS/MS targets to document synthetic cannabinoid intake in US military urine specimens. Clin. Chem. Lab. Med., 2015; 53: 423-434.

[62] Knittel JL, Holler JM, Chmiel JD, Vorce SP, Magluilo Jr J, Levine B, Ramos G, Bosy TZ. Analysis of parent synthetic cannabinoids in blood and urinary metabolites by liquid chromatography tandem mass spectrometry. J. Anal. Toxicol., 2016; 40: 173-186.

[63] Kronstrand R, Brinkhagen L, Birath-Karlsson C, Roman M, Josefsson M. LC-QTOF-MS as a superior strategy to immunoassay for the comprehensive analysis of synthetic cannabinoids in urine. Anal. Bioanal. Chem., 2014; 406: 3599-3609.

[64] Bertol E, Vaiano F, Di Milia MG, Mari F. In vivo detection of the new psychoactive substance AM-694 and its metabolites. Forensic Science International, 2015; 256: 21-27.

Table 1: List of the major metabolites identified in human urine samples. Characteristic fragment ions, accurate masses and elemental composition are given for each metabolite.

Metabolite and characteristic transitions	Monoisotopic accurate mass	Elemental composition	Error [ppm]	Retention time [min]
AM-2201:				
Monohydroxylated *N*-alkyl chain				7.1
molecular ion $[M+H]^+$ (*m/z* 376)	376.1707	$C_{25}H_{22}FNO_2$	-0.7	
fragment ion (*m/z* 155)	155.0484	$C_{11}H_7O$	4.81	
fragment ion (*m/z* 127)	127.0537	$C_{10}H_7$	4.18	
fragment ion (*m/z* 144)	144.044	C_9H_6NO	2.73	
Monohydroxylated indole moiety				7.3
molecular ion $[M+H]^+$ (*m/z* 376)	376.1706	$C_{25}H_{22}FNO_2$	0.36	
fragment ion (*m/z* 248)	248.1077	$C_{14}H_{15}FNO_2$	1.75	
fragment ion (*m/z* 160)	160.039	$C_9H_6NO_2$	1.92	
fragment ion (*m/z* 155)	155.0488	$C_{11}H_7O$	2.22	
fragment ion (*m/z* 127)	127.054	$C_{10}H_7$	1.8	
AM-694:				
Monohydroxylated *N*-alkyl side chain				6.4/6.6
molecular ion $[M+H]^+$ (*m/z* 452)	452.0516	$C_{20}H_{20}FINO_2$	0.28	
fragment ion (*m/z* 231)	230.9293	C_7H_4IO	3.63	
fragment ion (*m/z* 203)	202.9353	C_6H_4I	-0.4	
Hydrolytically defluorinated				6.7
molecular ion $[M+H]^+$ (m/z 434)	434.0611	$C_{20}H_{21}INO_2$	0	
fragment ion (*m/z* 231)	230.9296	C_7H_4IO	2.32	
fragment ion (*m/z* 203)	202.9353	C_6H_4I	-0.4	
fragment ion (*m/z* 186)	186.1277	$C_{13}H_{16}N$	0.14	
fragment ion (*m/z* 144)	144.0446	C_9H_6NO	-1.47	
N-Pentanoic acid metabolite				6.5
molecular ion $[M+H]^+$ (m/z 448)	448.0408	$C_{20}H_{19}INO_3$	-0.87	
fragment ion (*m/z* 244)	244.0969	$C_{14}H_{14}NO_3$	-0.33	
fragment ion (*m/z* 231)	230.9293	C_7H_4IO	3.63	
fragment ion (*m/z* 203)	202.9357	C_6H_4I	-2.38	
fragment ion (*m/z* 144)	144.0446	C_9H_6NO	-1.47	
JWH-007:				
Monohydroxylated *N*-alkyl chain				7.7/8.2
molecular ion $[M+H]^+$ (*m/z* 372)	372.1961	$C_{25}H_{26}NO_2$	-0.79	
fragment ion (*m/z* 244)	244.1336	$C_{15}H_{18}NO_2$	-1.62	
fragment ion (*m/z* 158)	158.0604	$C_{10}H_8NO$	-2.29	
fragment ion (*m/z* 155)	155.0492	$C_{11}H_7O$	-0.38	
fragment ion (*m/z* 127)	127.0541	$C_{10}H_7$	1	
N-Pentanoic acid metabolite				7.5
molecular ion $[M+H]^+$ (*m/z* 386)	386.175	$C_{25}H_{24}NO_3$	0.18	
fragment ion (*m/z* 258)	258.1131	$C_{15}H_{16}NO_3$	-2.45	
fragment ion (*m/z* 158)	158.0598	$C_{10}H_8NO$	1.53	

fragment ion (*m/z* 155)	155.0487	$C_{11}H_7O$	2.86	
fragment ion (*m/z* 127)	127.0539	$C_{10}H_7$	2.59	
Dihydroxylated *N*-alkyl chain				6.9
molecular ion $[M+H]^+$ (*m/z* 388)	388.191	$C_{25}H_{26}NO_3$	-0.72	
fragment ion (*m/z* 260)	260.1276	$C_{15}H_{18}NO_3$	2	
fragment ion (*m/z* 158)	158.0598	$C_{10}H_8NO$	1.53	
fragment ion (*m/z* 155)	155.0492	$C_{11}H_7O$	-0.38	
fragment ion (*m/z* 127)	127.0541	$C_{10}H_7$	1	
JWH-019:				
Monohydroxylated *N*-alkyl chain				7.2/8.0
molecular ion $[M+H]^+$ (*m/z* 372)	372.1958	$C_{25}H_{26}NO_2$	-0.23	
fragment ion (*m/z* 155)	155.0486	$C_{11}H_7O$	3.51	
fragment ion (*m/z* 127)	127.0536	$C_{10}H_7$	4.97	
N-Hexanoic acid metabolite				7.0
molecular ion $[M+H]^+$ (*m/z* 386)	386.1751	$C_{25}H_{24}NO_3$	-1.67	
fragment ion (*m/z* 155)	155.0488	$C_{11}H_7O$	2.22	
fragment ion (*m/z* 127)	127.0537	$C_{10}H_7$	4.18	
JWH-203:				
Monohydroxylated *N*-alkyl chain				7.2/7.7
molecular ion $[M+H]^+$ (*m/z* 356)	356.1412	$C_{21}H_{23}ClNO_2$	0.13	
fragment ion (*m/z* 125)	125.0147	C_7H_6Cl	4.47	
fragment ion (*m/z* 186)	186.1271	$C_{13}H_{16}N$	3.38	
fragment ion (*m/z* 204)	204.1379	$C_{13}H_{18}NO$	1.92	
fragment ion (*m/z* 144)	144.0801	C_9H_6NO	0.53	
Monohydroxylated indole moiety				8.3
molecular ion $[M+H]^+$ (*m/z* 356)	356.1412	$C_{21}H_{23}ClNO_2$	-1.59	
fragment ion (*m/z* 125)	125.0147	C_7H_6Cl	4.47	
fragment ion (*m/z* 204)	204.138	$C_{13}H_{18}NO$	1.43	
fragment ion (*m/z* 160)	160.0386	$C_9H_6NO_2$	4.43	
fragment ion (*m/z* 230)	230.1175	$C_{14}H_{16}NO_2$	0.24	
N-Pentanoic acid metabolite				7.0
molecular ion $[M+H]^+$ (*m/z* = 370)	370.1204	$C_{21}H_{21}ClNO_3$	1.03	
fragment ion (*m/z* 125)	125.0147	C_7H_6Cl	4.47	
fragment ion (*m/z* 200)	200.1061	$C_{13}H_{14}NO$	4.47	
fragment ion (*m/z* 144)	144.0809	C_9H_6NO	2.63	
fragment ion (*m/z* 218)	218.1184	$C_{13}H_{16}NO_2$	-3.89	
fragment ion (*m/z* 244)	244.0965	$C_{14}H_{14}NO_3$	-2.8	
JWH-307:				
Monohydroxylated 2-fluoro-phenyl pentyl pyrrol moiety				8.2/8.5
molecular ion $[M+H]^+$ (*m/z* 402)	402.1864	$C_{26}H_{25}FNO_2$	0.38	
fragment ion (*m/z* 230)	230.1329	$C_{15}H_{17}FN$	4.6	
fragment ion (*m/z* 155)	155.0484	$C_{11}H_7O$	4.81	
Dihydrodiol-naphthyl metabolites				8.1
molecular ion $[M+H]^+$ (*m/z* 420)	420.1967	$C_{26}H_{27}FNO_3$	0.59	

fragment ion (*m/z* 258)	258.1283	$C_{16}H_{17}FNO$	2.21	
fragment ion (*m/z* 189)	189.0543	$C_{11}H_9O_3$	1.7	
fragment ion (*m/z* 171)	171.0437	$C_{11}H_7O_2$	2.09	
fragment ion (*m/z* 161)	161.06	$C_{10}H_9O_2$	-1.84	
fragment ion (*m/z* 143)	143.0491	$C_{10}H_7O$	0	
Hydroxylated at naphthyl and 2-fluoro-phenyl pentyl pyrrol moieties				6.9/7.2
molecular ion $[M+H]^+$ (*m/z* 418)	418.1813	$C_{26}H_{25}FNO_3$	-0.51	
fragment ion (*m/z* 248)	248.1435	$C_{15}H_{19}FNO$	4.12	
fragment ion (*m/z* 230)	230.1339	$C_{15}H_{17}FN$	0.24	
fragment ion (*m/z* 171)	171.0435	$C_{11}H_7O_2$	3.3	
MAM-2201:				
Monohydroxylated indole moiety				7.9
molecular ion $[M+H]^+$ (*m/z* 390)	390.1863	$C_{25}H_{25}FNO_2$	0.21	
fragment ion (*m/z* 248)	248.1076	$C_{14}H_{15}FNO_2$	2.16	
fragment ion (*m/z* 169)	169.0644	$C_{12}H_9O$	2.33	
fragment ion (*m/z* 160)	160.0392	$C_9H_6NO_2$	0.66	
Monohydroxylated naphthyl moiety				7.5
molecular ion $[M+H]^+$ (*m/z* 390)	390.1862	$C_{25}H_{25}FNO_2$	0.47	
fragment ion (*m/z* 232)	232.1128	$C_{14}H_{15}FNO$	1.81	
fragment ion (*m/z* 185)	185.0596	$C_{12}H_9O_2$	0.58	
fragment ion (*m/z* 144)	144.0446	C9H6NO	-1.47	
N-Pentanoic acid metabolite				7.8
molecular ion $[M+H]^+$ (*m/z* = 386)	386.1747	$C_{25}H_{24}NO_3$	0.96	
fragment ion (*m/z* 169)	169.0647	$C_{12}H_9O$	0.54	
fragment ion (*m/z* 144)	144.0444	C_9H_6NO	-0.07	
fragment ion (*m/z* 141)	141.0696	$C_{11}H_9$	1.98	
UR-144:				
Monohydroxylated *N*-alkyl chain of the ring opened isomer				7.9
molecular ion $[M+H]^+$ (*m/z* 328)	328.2273	$C_{21}H_{30}NO_2$	-0.59	
fragment ion (*m/z* 230)	230.1176	$C_{14}H_{16}NO_2$	0	
fragment ion (*m/z* 144)	144.0441	C_9H_6NO	2.03	
Monohydroxylated *N*-alkyl side chain				8.3/8.8
molecular ion $[M+H]^+$ (*m/z* 328)	328.2268	$C_{21}H_{30}NO_2$	0.93	
fragment ion (*m/z* 230)	230.1176	$C_{14}H_{16}NO_2$	0	
fragment ion (*m/z* 125)	125.0963	$C_8H_{13}O$	-1.68	
Monohydroxylated tetra methyl cyclopropyl moiety				9.2
molecular ion $[M+H]^+$ (*m/z* 328)	328.2272	$C_{21}H_{30}NO_2$	-0.29	
fragment ion (*m/z* 214)	214.1221	$C_{14}H_{16}NO$	2.54	
fragment ion (*m/z* 144)	144.0447	C_9H_6NO	-2.17	
XLR-11:				
N-Pentanoic acid metabolite of the ring opened isomer				7.8
molecular ion $[M+H]^+$ (*m/z* 342)	342.2074	$C_{21}H_{28}NO_3$	-3	
fragment ion (*m/z* 244)	244.0977	$C_{14}H_{14}NO_3$	-3.8	
fragment ion (*m/z* 144)	144.0447	C_9H_6NO	-2.2	

Tetra methyl cyclopropyl carboxylic acid metabolite				7.6
molecular ion $[M+H]^+$ (*m/z* 360)	360.1966	$C_{21}H_{27}FNO_3$	0.9	
fragment ion (*m/z* 232)	232.1136	$C_{14}H_{15}FNO$	-1.5	
fragment ion (*m/z* 144)	144.0447	C_9H_6NO	-2	

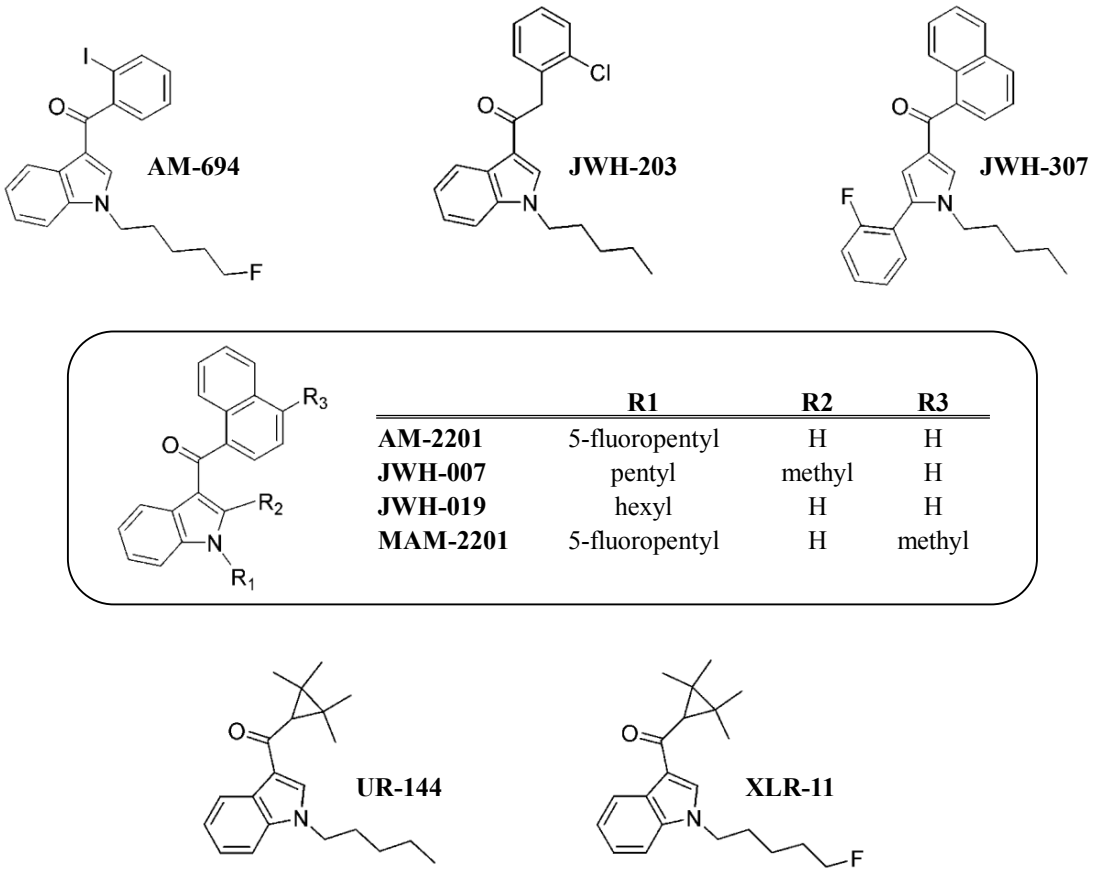

	R1	R2	R3
AM-2201	5-fluoropentyl	H	H
JWH-007	pentyl	methyl	H
JWH-019	hexyl	H	H
MAM-2201	5-fluoropentyl	H	methyl

Figure 1. Chemical structures of the synthetic cannabinoids investigated.

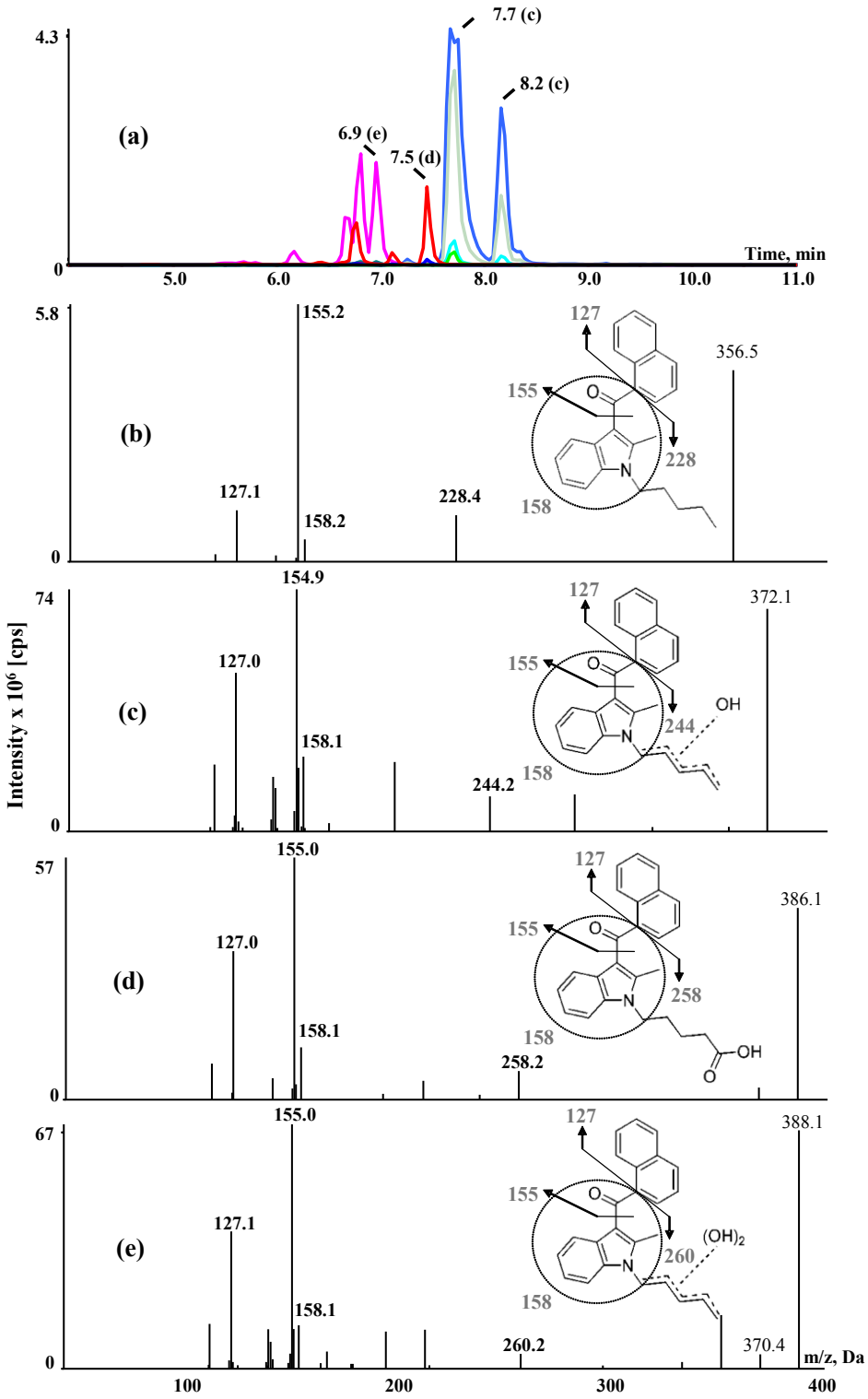

Figure 2: MRM chromatogram of the urinary metabolites (a) and ESI(+) MS/MS spectra of the parent compound JWH-007 (b), the two metabolites monohydroxylated at the *N*-alkyl chain (c), the *N*-pentanoic acid metabolite (d) and the metabolite dihydroxylated at the *N*-alkyl side chain (e). The ion traces corresponding to the *m/z* values printed in bold are depicted in the MRM chromatogram. Different collision energies were used in MRM mode (a) and EPI mode (b)-(e).

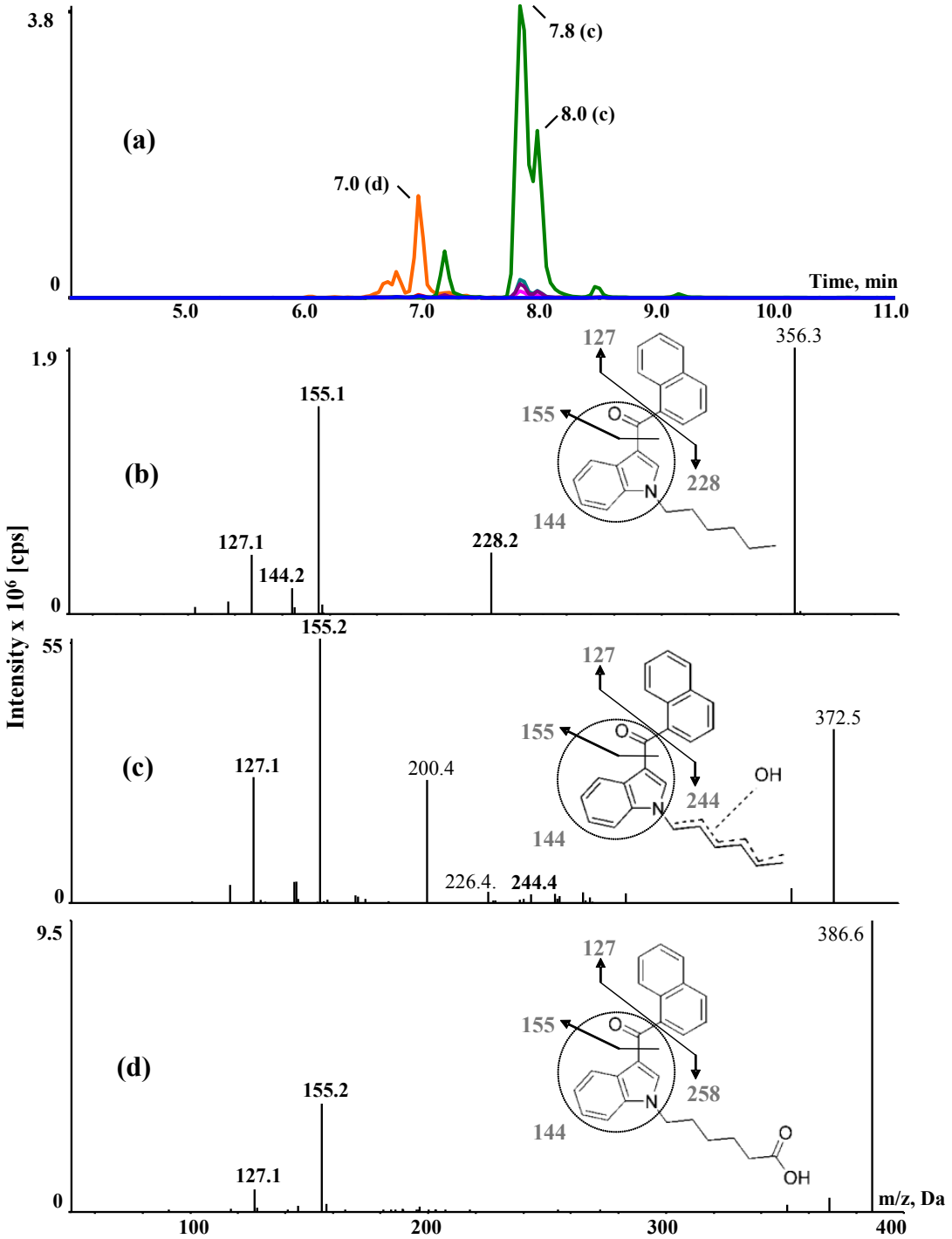

Figure 3: MRM chromatogram of the urinary metabolites (a) and ESI(+) MS/MS spectra of the parent compound JWH-019 (b), the two metabolites monohydroxylated at the *N*-alkyl chain (c) and the *N*-hexanoic acid metabolite (d). The ion traces corresponding to the *m/z* values printed in bold are depicted in the MRM chromatogram. Different collision energies were used in MRM mode (a) and EPI mode (b)-(d).

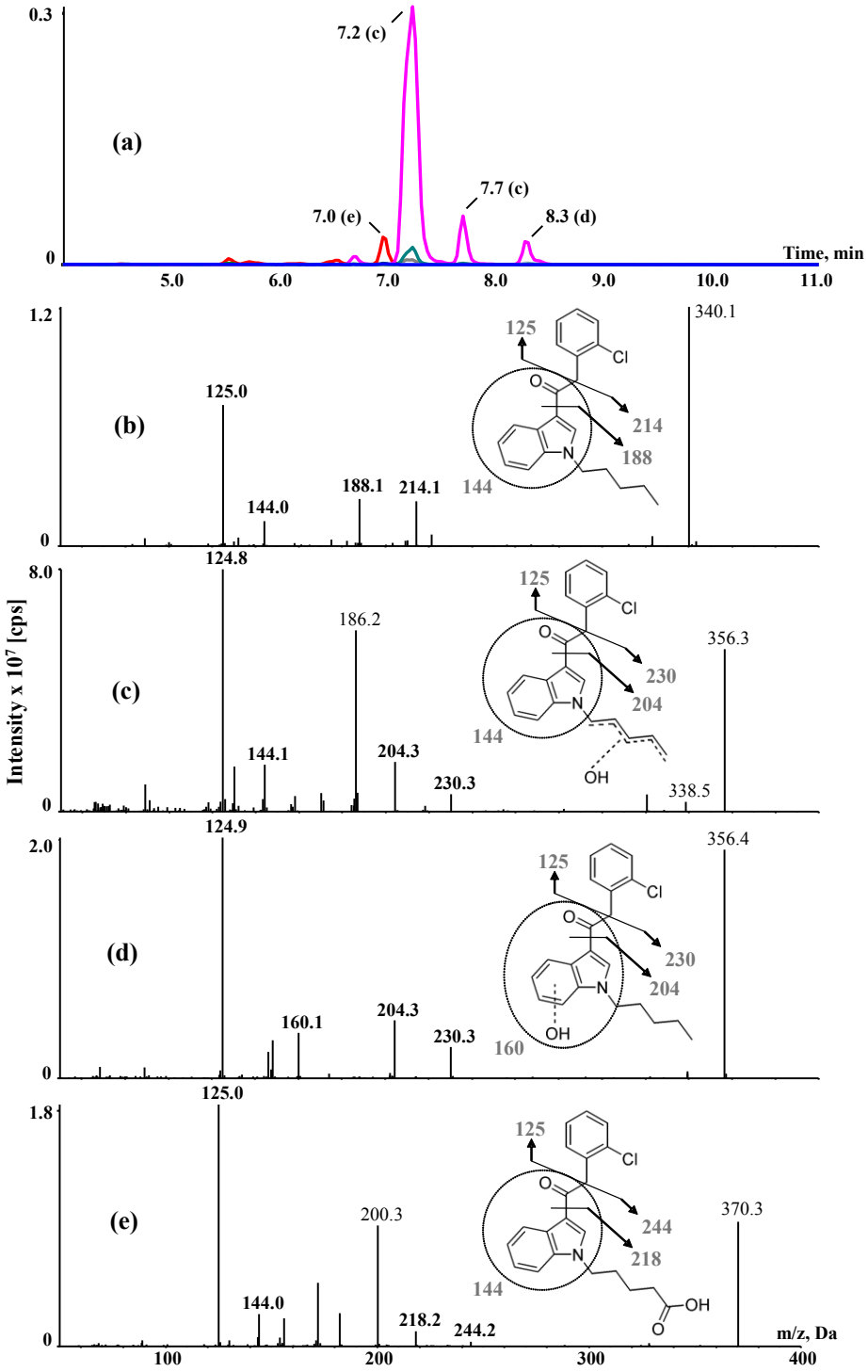

Figure 4: MRM chromatogram of the urinary metabolites (a) and ESI(+) MS/MS spectra of the parent compound JWH-203 (b), the two metabolites monohydroxylated at the *N*-alkyl chain (c), the metabolite monohydroxylated at the indole moiety (d) and the *N*-pentanoic acid metabolite (e). The ion traces corresponding to the *m/z* values printed in bold are depicted in the MRM chromatogram. Different collision energies were used in MRM mode (a) and EPI mode (b)-(e).

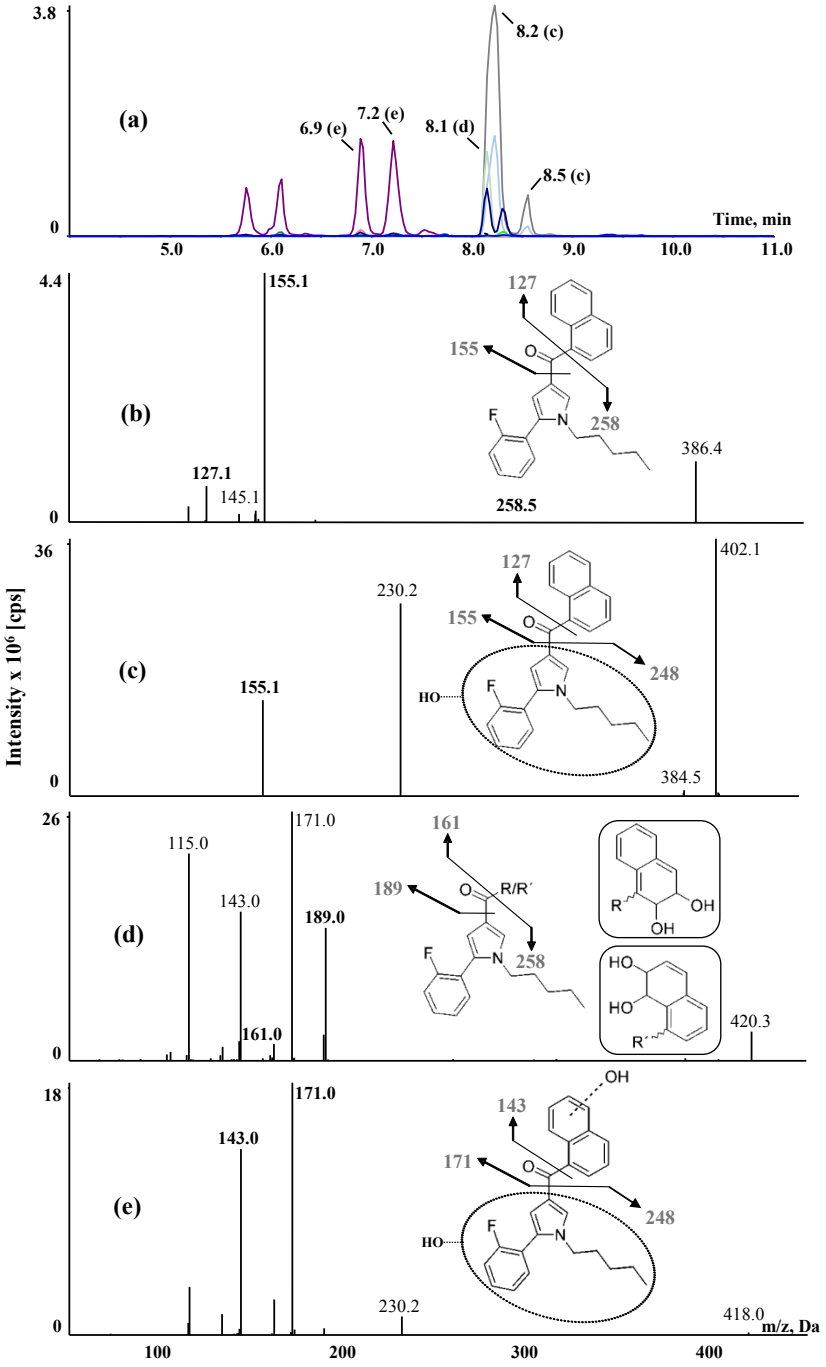

Figure 5: MRM chromatogram of the urinary metabolites (a) and ESI(+) MS/MS spectra of the parent compound JWH-307 (b), the two metabolites monohydroxylated at the 2-fluoro-phenyl pentyl pyrrol moiety (c), a dihydrodiol metabolite at the naphthyl moiety (d) and the two metabolites dihydroxylated at the naphthyl and 2-fluoro-phenyl pentyl pyrrol moieties (e). The ion traces corresponding to the *m/z* values printed in bold are depicted in the MRM chromatogram. Different collision energies were used in MRM mode (a) and EPI mode (b)-(e).

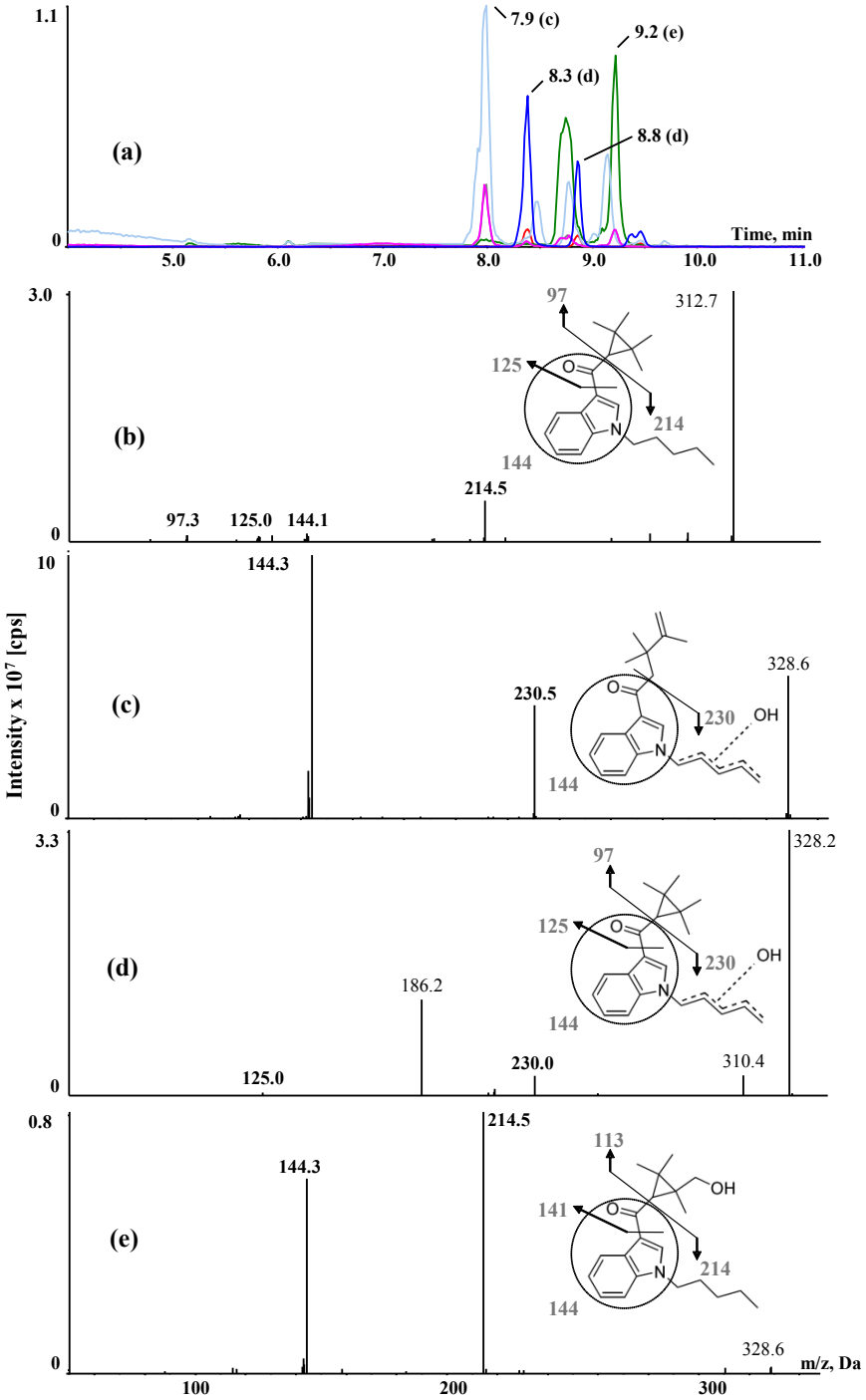

Figure 6: MRM chromatogram of the urinary metabolites (a) and ESI(+) MS/MS spectra of the parent compound UR-144 (b), the metabolite of the ring opened isomer monohydroxylated at the *N*-alkyl side chain (c), the two metabolites monohydroxylated at the *N*-alkyl side chain (d) and the metabolite monohydroxylated at the tetra methyl cyclopropyl moiety (e). The ion traces corresponding to the *m/z* values printed in bold are depicted in the MRM chromatogram. Different collision energies were used in MRM mode (a) and EPI mode (b)-(e).

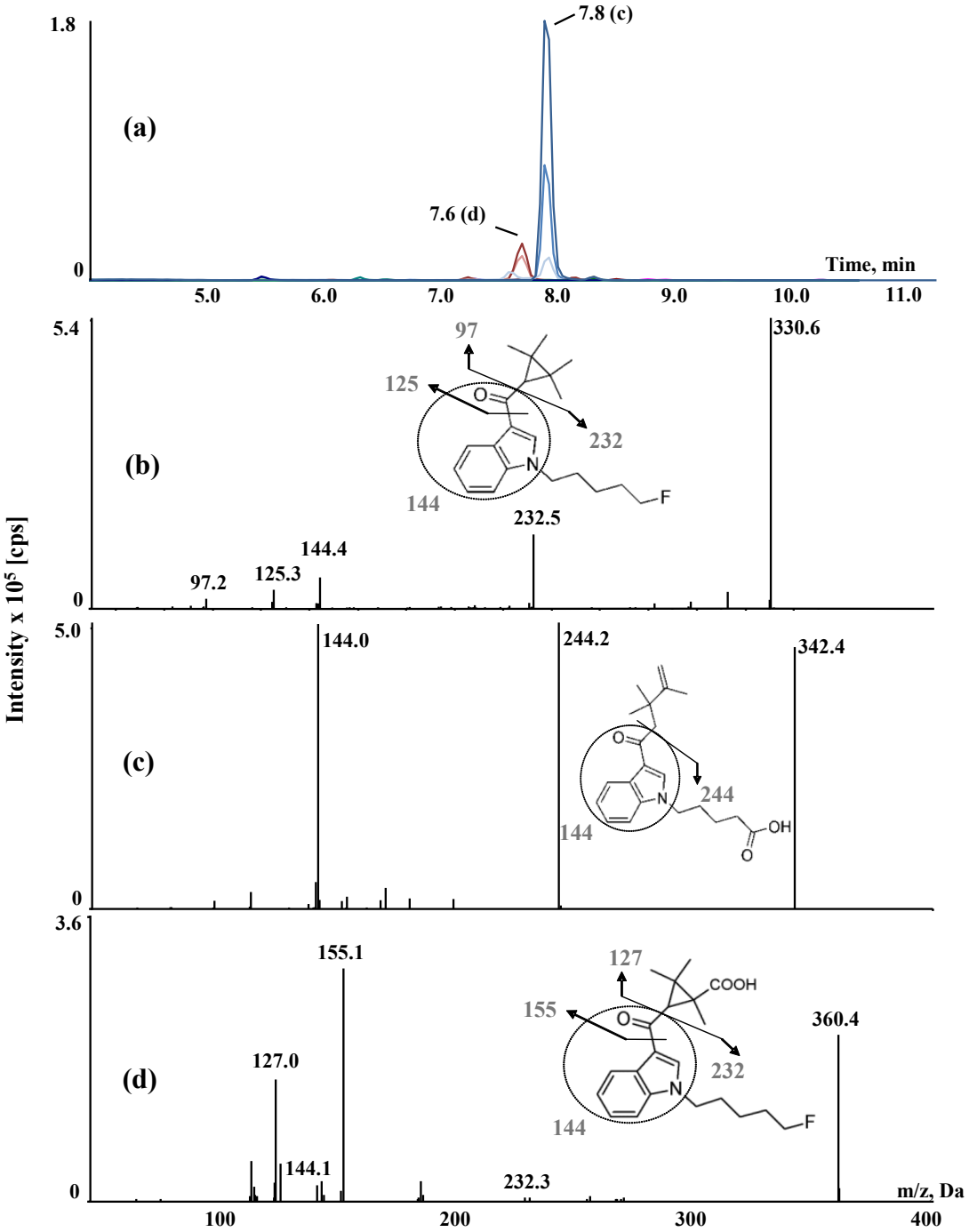

Figure 7: MRM chromatogram of the urinary metabolites (a) and ESI(+) MS/MS spectra of the parent compound XLR-11 (b), the *N*-pentanoic acid metabolite of the ring opened isomer (c) and a tetra methyl cyclopropyl carboxylic acid metabolite (d). The ion traces corresponding to the *m/z* values printed in bold are depicted in the MRM chromatogram. Different collision energies were used in MRM mode (a) and EPI mode (b)-(d).

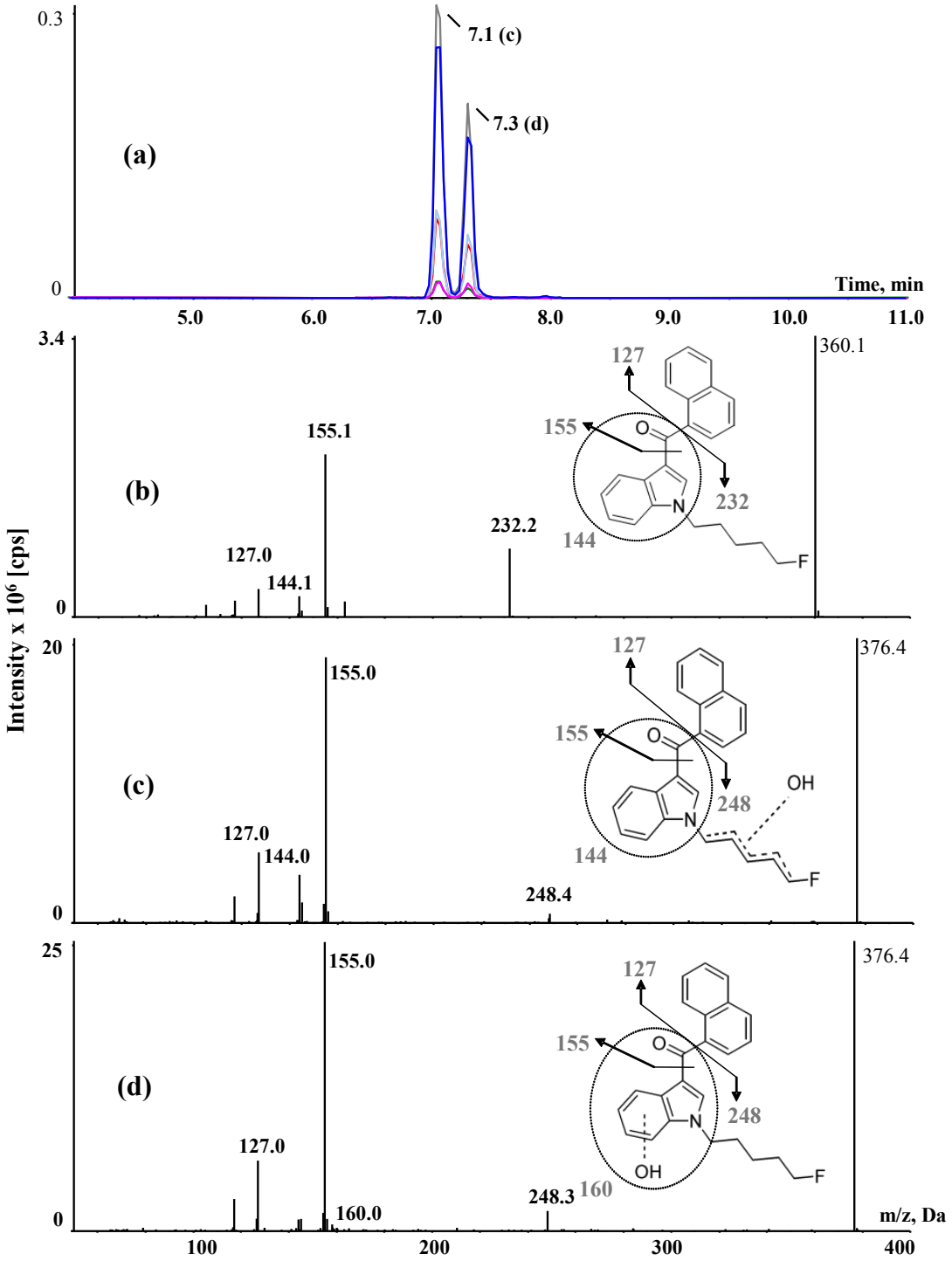

Figure 8: MRM chromatogram of the urinary metabolites (a) and ESI(+) MS/MS spectra of the parent compound AM-2201 (b), the metabolite monohydroxylated at the *N*-alkyl side chain (c) and the metabolite monohydroxylated at the indole moiety (d). The ion traces corresponding to the *m/z* values printed in bold are depicted in the MRM chromatogram. Different collision energies were used in MRM mode (a) and EPI mode (b)-(d).

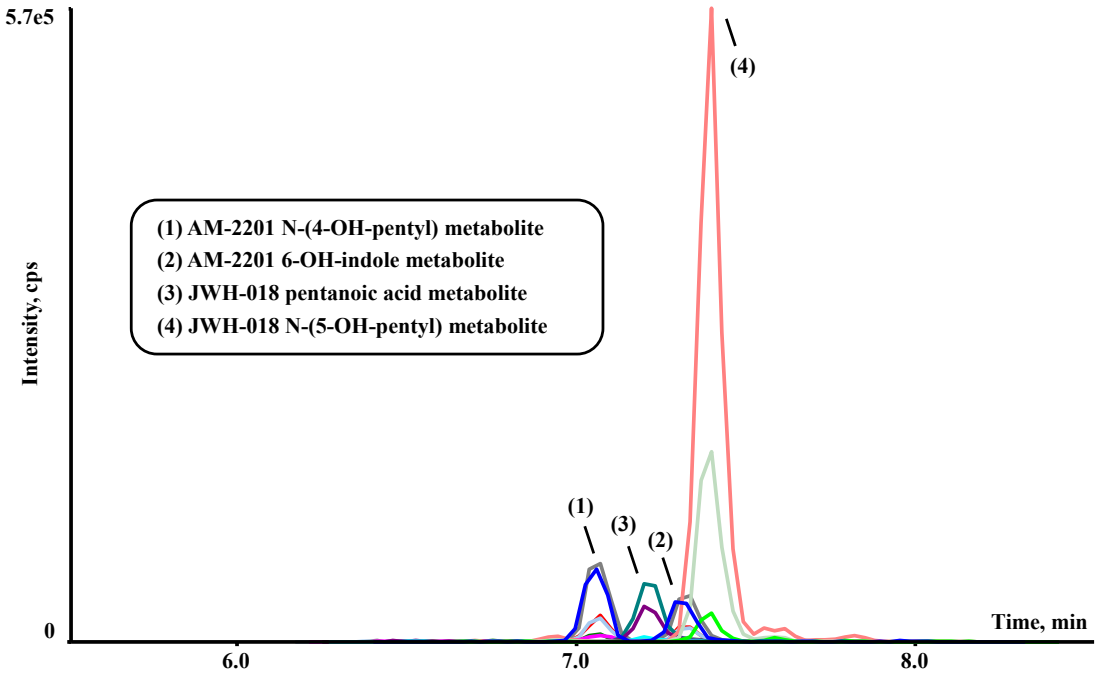

Figure 9: MRM chromatogram of a human urine sample positive for AM-2201.

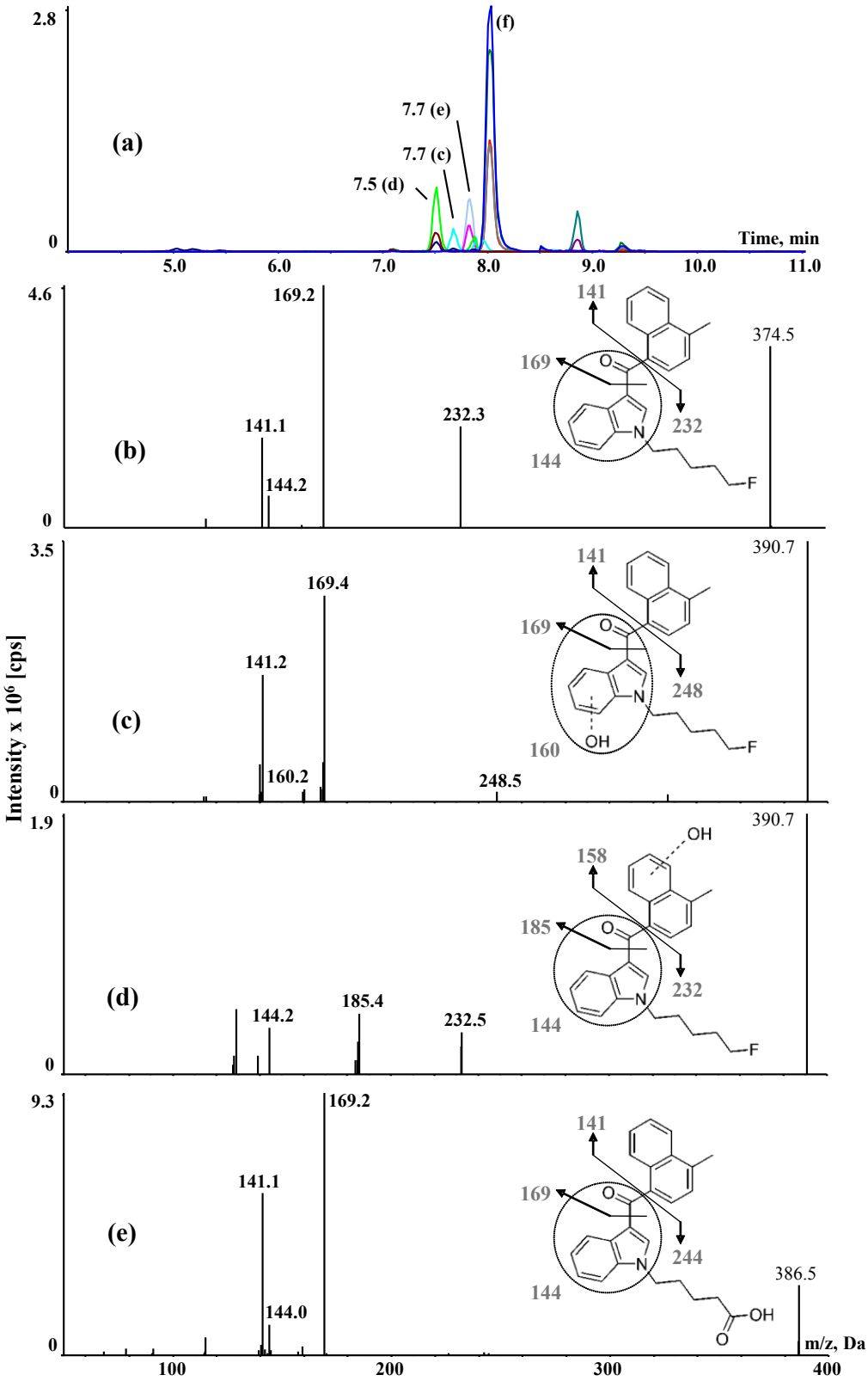

Figure 10: MRM chromatogram of the urinary metabolites (a) and ESI(+) MS/MS spectra of the parent compound MAM-2201 (b), the metabolite monohydroxylated at the indole moiety (c), the metabolite monohydroxylated at naphthyl moiety (d) and the *N*-pentanoic acid metabolite (e). The ion traces corresponding to the *m/z* values printed in bold are depicted in the MRM chromatogram. Different collision energies were used in MRM mode (a) and EPI mode (b)-(e).

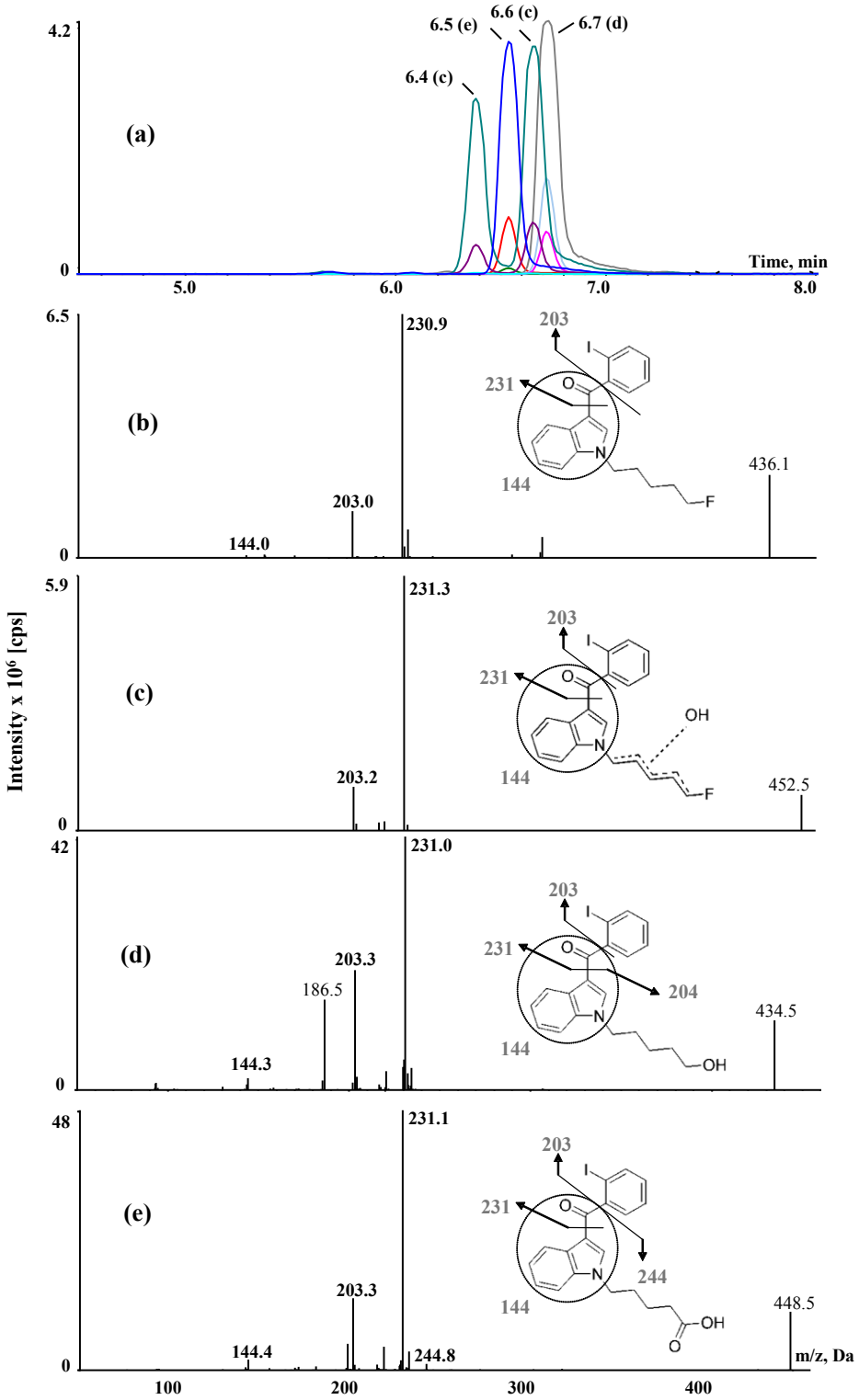

Figure 11: MRM chromatogram of the urinary metabolites (a) and ESI(+) MS/MS spectra of the parent compound AM-694 (b), the two metabolite monohydroxylated at the *N*-alkyl side chain (c), the metabolite formed by hydrolytic defluorination (d) and the *N*-pentanoic acid metabolite (e). The ion traces corresponding to the *m/z* values printed in bold are depicted in the MRM chromatogram. Different collision energies were used in MRM mode (a) and EPI mode (b)-(e).